Inorganic Chemistry

Article

pubs.acs.org/IC

Electrocatalytic H_2 Evolution by Supramolecular Ru^{II}–Rh^{III}–Ru^{II} Complexes: Importance of Ligands as Electron Reservoirs and Speciation upon Reduction

Gerald F. Manbeck,*[,†] Theodore Canterbury, Rongwei Zhou, Skye King, Geewoo Nam, and Karen J. Brewer[‡]

Department of Chemistry, Virginia Tech, Blacksburg, Virginia 24061, United States

Supporting Information

ABSTRACT: The supramolecular water reduction photocatalysts $[\{(Ph_2phen)_2Ru(dpp)\}_2RhX_2](PF_6)_5$ (Ph_2phen = 4,7-diphenyl-1,10-phenanthroline, dpp =2,3-bis(2-pyridyl)pyrazine X = Cl, Br) are efficient electrocatalysts for the reduction of CF_3SO_3H, CF_3CO_2H, and CH_3CO_2H to H_2 in DMF or DMF/H_2O mixtures. The onset of catalytic current occurs at −0.82 V versus Ag/AgCl for CF_3SO_3H, −0.90 V for CF_3CO_2H, and −1.1 V for CH_3CO_2H with overpotentials of 0.61, 0.45, and 0.10 V, respectively. In each case, catalysis is triggered by the first dpp ligand reduction implicating the dpp as an electron reservoir in catalysis. A new species with $E_{pc} \sim -0.75$ V was observed in the presence of stoichiometric amounts of strong acid, and its identity is proposed as the $Rh(H)^{III/II}$ redox couple. H_2 was produced in 72−85% Faradaic yields and 95−116 turnovers after 2 h and 435 turnovers after 10 h of bulk electrolysis. The identities of Rh(I) species upon reduction have been studied. In contrast to the expected dissociation of halides in the Rh(I) state, the halide loss depends on solvent and water content. In dry CH_3CN, in which Cl^- is poorly solvated, a [Ru] complex dissociates and $[(Ph_2phen)_2Ru(dpp)Rh^ICl_2]^+$ and $[(Ph_2phen)_2Ru(dpp)]^{2+}$ are formed. In contrast, for X = Br^-, the major product of reduction is the intact trimetallic Rh(I) complex $[\{(Ph_2phen)_2Ru(dpp)\}_2Rh^I]^{5+}$. Chloride loss in CH_3CN is facilitated by addition of 3 M H_2O. In DMF, the reduced species is $[\{(Ph_2phen)_2Ru(dpp)\}_2Rh^I]^{5+}$ regardless of X = Cl^- or Br^-.

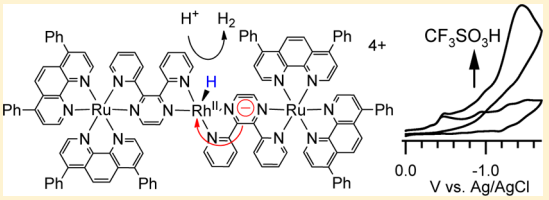

INTRODUCTION

Artificial photosynthesis (AP) for the storage of solar energy in the form of chemical bonds is a promising route to renewable fuels such as H_2 or reduced carbon dioxide.[1−6] A molecular approach to hydrogen production via AP is attractive since molecules for light harvesting, charge separation, and catalysis can first be optimized for each function;[7−12] however, practical application will require immobilization of each component and integration into a device. The supramolecular approach, in which components are covalently linked, is a step toward a device since diffusion controlled bimolecular electron transfer (ET) reactions are eliminated. Ideally, the supramolecule should facilitate accumulation of multiple charge carriers allowing catalysis of multielectron reactions, i.e., the two-electron reduction of water to hydrogen.[13]

The search for effective hydrogen production chromophore-catalyst supramolecules has revealed dinuclear Ru-cobaloximes;[14,15] self-assembled photosystem I cobaloxime hybrids;[16] tetrametallic Ru_3–Pt complexes;[17] bimetallic varietals of Ru–Pt,[18] Ir–Co,[19] Ru–Pd,[20] Ru–Rh;[21] zinc porphyrin-cobaloximes;[22] and Ru^{II}–Rh^{II}–Ru^{II} complexes studied by the Brewer group and others.[23−29] Trimetallic supramolecules $[\{(TL)_2Ru(dpp)\}_2RhX_2]^{5+}$ (TL = terminal bidentate ligand, dpp = 2,3-bis(2-pyridyl)pyrazine, and X = Cl, Br) are promising photocatalysts operating through photoinitiated electron collected at Rh via the two cycles of the following sequence: Ru(dπ) → dpp(π^*) MLCT (metal-to-ligand charge transfer) excitation, reductive quenching of the triplet state, and intramolecular ET to Rh. Similar to $[Rh(bpy)_2Cl_2]^+$, sequential ET presumably triggers halide loss to generate vacant sites for catalysis.[30] Subsequent steps in the mechanism are poorly understood although recent theoretical work on mononuclear $[Rh^{III}(Me_2\text{-}bpy)_2Cl_2]^+$ may provide some insight into the supramolecule behavior.[31] Key questions include the potentials of important hydride redox couples, the rate of ET for the second electron, the influence of dissociated ligands in the catalytic cycle, the reversibility of H_2 release, and solvent effects on speciation.

Hydrogen production catalysts are often evaluated under electrocatalytic conditions since solar fuels can be produced by electrolysis powered by photovoltaics.[32−58] Regarding mechanistic insight, cyclic voltammetry (CV) enables catalyst screening and scrutiny in the absence of complications associated with photochemical studies.[59] CV data yield rates, overpotentials, and redox potentials of putative intermediates unobservable in photocatalysis. Again, the issue of mass transport has prompted the invention of electrode materials modified by molecular catalysts.[60−65] This approach provides a remarkable improvement in efficiency, overpotential, and

Received: July 9, 2015
Published: August 6, 2015

DOI: 10.1021/acs.inorgchem.5b01536
Inorg. Chem. 2015, 54, 8148−8157

durability as shown by the 55 000 turnovers in water using cobaloxime catalysts[60] or 100 000 turnovers for Ni bis-diphosphosphine catalysts[61,62] grafted on carbon nanotubes. Photocathodes modified with molecular catalysts provide a method to drive reductive reactions with solar input.[65−67] An emerging advanced design entails dye-sensitized photocathodes such as p-type NiO[68−71] in which charge injection occurs from the semiconductor valence band into the excited state of the dye, thereby eliminating the sacrificial electron donors commonly used for exploratory research.

The supramolecular Ru^{II}−Rh^{III} or Ru^{II}−Rh^{III}−Ru^{II} moieties proven efficient for photocatalysis are ideally suited for surface-confined photoelectrochemical hydrogen production, and the ^{3}MLCT excited state of the $[(TL)_2Ru(dpp)]^{2+}$ chromophore is a sufficiently strong oxidizing and reducing agent to split water. To date, no electrocatalytic studies have been undertaken using these motifs. While electrocatalytic hydrogen production is known for several Rh catalysts such as $[(C_5Me_5)Rh(bpy)Cl]^+$,[72−75] *trans*-$RhCl(CO)(PPh_3)_2$,[76] and Rh^I(TPP) (TPP = 5,10,15,20-tetraphenylporphyrin),[77] it is anticipated that the unique electronics of the dpp bridging ligand bound to Ru(II) may provide reactivity different from simple models such as $[Rh(bpy)_2Cl_2]^+$ or $[Rh(dpp)_2Cl_2]^+$.

As an initial study prior to surface confinement, we sought to verify homogeneous electrocatalytic proton reduction using $[\{(Ph_2phen)_2Ru(dpp)\}_2RhX_2]^{5+}$ (X = Br (**1Br$_2$**), Cl (**1Cl$_2$**), Figure 1) in DMF, and to gain understanding of the

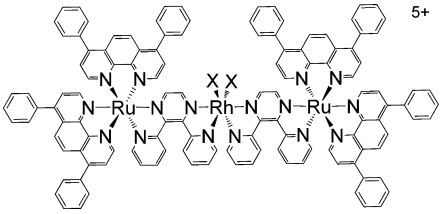

Figure 1. Representation of $[\{(Ph_2phen)_2Ru(dpp)\}_2RhX_2]^{5+}$ (X = Cl (**1Cl$_2$**), Br (**1Br$_2$**); Ph_2phen = 4,7-diphenyl-1,10-phenanthroline; dpp = 2,3-bis(2-pyridyl)pyrazine).

mechanism. Catalytic waveforms are strongly dependent on acid pK_a, and suggest a mechanism in which H_2 is released by protonation of a Rh(II) hydride with one reduced dpp ligand. Importantly, this mechanism allows speculation regarding the photochemical reaction since the dpp reduction is accessible by reductive excited state quenching. Hydrogen release is then a "dark reaction" consistent with previous reports of concentration-dependent turnover numbers.[78] Analysis of reduced species reveals an unexpected solvent-dependent speciation in which the reduced Rh(I) trimetallic remains intact only if halide dissociation is facilitated by its solubility. If the halide is insoluble in the reaction medium, a $[Ru(Ph_2phen)_2(dpp)]^{2+}$ unit dissociates in contrast to halide loss.

RESULTS

Cyclic Voltammetry in DMF. The reductive CV of $[\{(Ph_2phen)_2Ru(dpp)\}_2RhBr_2]^{5+}$ in DMF features overlapping irreversible $Rh^{III/II}$ and $Rh^{II/I}$ couples at −0.34 V versus Ag/AgCl (Figure 2, peak 1) and two $dpp^{0/-}$ couples at E_p^c = −0.87 V (quasireversible, peak 2) and $E_{1/2}$ = −1.22 V (peak 3). Peak 4 at −1.47 V is assigned as a second reduction ($dpp^{-/2-}$) of one bridging ligand based on the ca. 0.5 V difference from the first dpp reduction.[79] CV data for $[\{(Ph_2phen)_2Ru(dpp)\}_2RhCl_2]^{5+}$ are similar with the exception of peak 1 appearing at −0.42 V.

CVs of **1Br$_2$** with 0, 5, 10, and 25 equiv of CF_3CO_2H are shown in Figure 2A. Addition of acid did not influence the $Rh^{III/II/I}$ wave or ligand-based couples; however, peak 5 appeared at −0.75 V prior to the first $dpp^{0/-}$ reduction. For ≥5 equiv of acid the current at −0.75 V remained unchanged, and catalytic current was observed at −0.9 V. The catalytic current peaked at −1.3 V for 10 equiv of CF_3CO_2H and at −1.6 V for 25 equiv. CVs for the reduction of CF_3CO_2H using **1Cl$_2$** (Figure S3) are nearly identical to those with **1Br$_2$**. The current enhancement, expressed as the ratio of peak current (i_c) to the current of the $dpp^{0/-}$ couple in the absence of acid (i_p), is 4.1 for **1Br$_2$** and 3.4 for **1Cl$_2$** complex in the presence of 10 equiv of acid. The thermodynamic potential for CF_3CO_2H reduction in DMF is −0.45 V versus Ag/AgCl.[80] Therefore, the onset of catalysis at −0.9 V for **1Br$_2$** represents an overpotential of 0.45 V.

CVs in the presence of CF_3SO_3H (E_{HA}° = −0.21 V vs Ag/AgCl)[81] were studied to examine the catalytic reduction of a stronger acid (Figure 2B). At low acid concentrations, peak 5 appeared at −0.62 V, and catalysis was triggered at −0.82 V. The current peaked at −1.3 V for 25 equiv of acid. Comparable CVs using **1Cl$_2$** as the catalyst were obtained. For 10 equiv of CF_3SO_3H, i_c/i_p = 3.5 and 3.4 for **1Br$_2$** and **1Cl$_2$**, respectively. Catalysis beginning at −0.82 V represents a 0.61 V overpotential for the reduction of CF_3SO_3H.

Weak acid behavior was examined using acetic acid (E_{HA}° = −1.0 V).[81] As shown in Figure 2C, a catalytic wave appeared

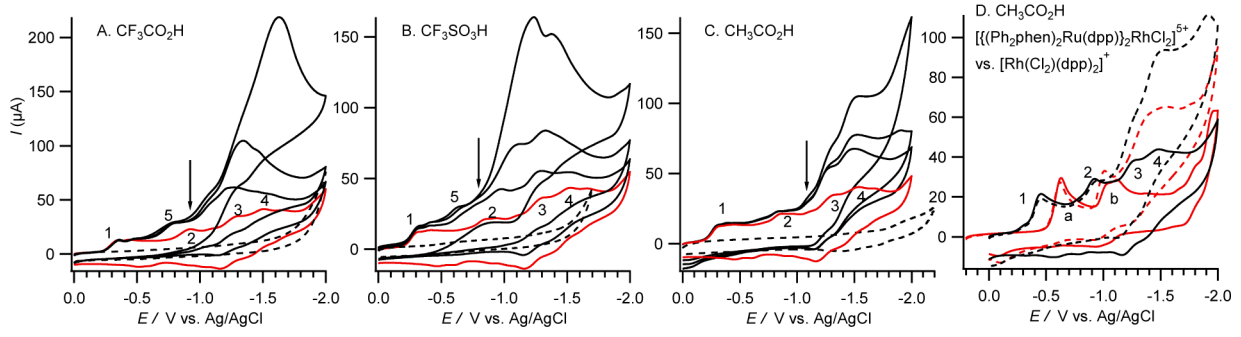

Figure 2. Cyclic voltammograms of 1.0 mM $[\{(Ph_2phen)_2Ru(dpp)\}_2RhBr_2]^{5+}$ in DMF/0.1 M Bu_4NPF_6 with 0, 5, 10, and 25 equiv of CF_3CO_2H (A), CF_3SO_3H (B), and CH_3CO_2H (C). In each plot, the CV in the absence of catalyst is shown for 22 mM acid, and the arrow indicates the onset of catalysis. Plot D compares CVs of 1.0 mM trimetallic $[\{(Ph_2phen)_2Ru(dpp)\}_2RhCl_2]^{5+}$ (black) and $[Rh(dpp)_2Cl_2]^+$ (red) in the absence (solid lines) and presence (dashed lines) of 10 equiv of CH_3CO_2H.

DOI: 10.1021/acs.inorgchem.5b01536
Inorg. Chem. 2015, 54, 8148−8157

with an onset potential near −1.1 V. In this case, the $dpp^{0/-}$ couple was observed as a shoulder on the catalytic wave at −1.23 V. The catalytic current appeared to plateau at −1.5 V for moderate acid concentrations. At 10 or more equiv of acid, a third peak appeared at −1.9 V. For 25 equiv of acid, i_c/i_p = 4.5 for **1Br$_2$** and 4.3 for **1Cl$_2$**. At the onset of catalysis at −1.05 V for acetic acid reduction, the overpotential is only 0.05 V.

Catalysis by [Rh(dpp)$_2$Cl$_2$]PF$_6$. The merit of Ru^{II}–Rh^{III}–Ru^{II} supramolecules as electrocatalysts lies in the photophysical properties of the appended Ru(II) chromophores and potential application in photoelectrocatalysis. Nevertheless, electrocatalysis using some *cis*-$Rh^{III}Cl_2$ monometallic precatalysts was examined for comparative purposes. No catalysis was observed for $[Rh(bpy)_2Cl_2]^+$. Since the electronic properties of dpp are somewhat different from bpy, $[Rh(dpp)_2Cl_2]^+$ was also studied. As shown in Figure 2D, **1Cl$_2$** exhibits greater activity for CH_3CO_2H reduction compared to $[Rh(dpp)_2Cl_2]^+$ (i_c/i_p = 3.3 and 2.1, respectively). Current for $[Rh(dpp)_2Cl_2]^+$ did not increase beyond 10 equiv of acid. Reduction of CF_3CO_2H is compared in Figure S4. For 10 equiv of acid, and potentials less negative than −1 V, the $[Rh(dpp)_2Cl_2]^+$ exhibited slightly more current than **1Cl$_2$**. Beyond a −1 V bias, **1Cl$_2$** holds clear advantage. While current for $[Rh(dpp)_2Cl_2]^+$ continued to increase beyond 10 equiv in this case, the increase is cathodic of −1 V, and the curve-cross at this potential was maintained for higher acid concentrations.

Cyclic Voltammetry in DMF/H$_2$O. Catalytic proton reduction experiments in pure organic solvents provide a starting point for analysis; however, water is the ideal medium for H_2 production.[48,49,52,53,82−84] Recently, efficient photocatalysis has been reported in pure water using similar multimetallic complexes.[85] Catalysis by $[\{(Ph_2phen)_2Ru(dpp)\}_2RhX_2]^{5+}$ was examined using 5% or 10% water in DMF acidified with CF_3SO_3H, CF_3CO_2H, or CH_3CO_2H (Figure 4).

In DMF/5% H_2O, the reductive CV of **1Br$_2$** was similar to the CV in pure DMF. Upon addition of CF_3SO_3H, a catalytic wave appeared at onset −1 V (Figure 3A). At the peak potential of −1.45 V, i_c/i_p = 5.3 for 10 equiv of acid. Without water, i_c/i_p = 3.5 at the peak potential of −1.3 V. At higher acid concentrations, direct reduction at the electrode begins to contribute to the current at −1.4 V. Experiments in DMF/10% water indicated adsorption of the reduced complex to the electrode at potentials cathodic of −1.2 V, and significant background current was observed beyond −1.2 V. Without added acid, the $dpp^{0/-}$ couples were obscured by the reduction of water as the proton source; however, current was low indicating a slow reaction (Figure 3B). With CF_3SO_3H, current increased at −1 V, but the high water content decreases catalytic activity compared to the 5% water solution. In the mixed 5% water in DMF solution, CVs with CF_3CO_2H are similar to those obtained in pure DMF (Figure 3C). As shown in Figure 3D, the catalyst is effective at similar potentials when the water content is increased to 10%. A new irreversible wave at −0.7 V was followed by peaks in current that shifted from −0.9 V at 5 equiv of acid to −1.3 V at 10 equiv of acid.

Figure 3E shows CVs of **1Br$_2$** in DMF/5% water with CH_3CO_2H. The CVs are similar to those without H_2O with the exception of higher i_c/i_p ratios at E_p. Without H_2O, for 15 equiv of CH_3CO_2H, i_c/i_p = 3.8 for **1Br$_2$** and 3.5 for **1Cl$_2$**. With 5% H_2O, i_c/i_p increased to 6.1 and 6.4, respectively, indicating enhanced catalysis in the presence of water.

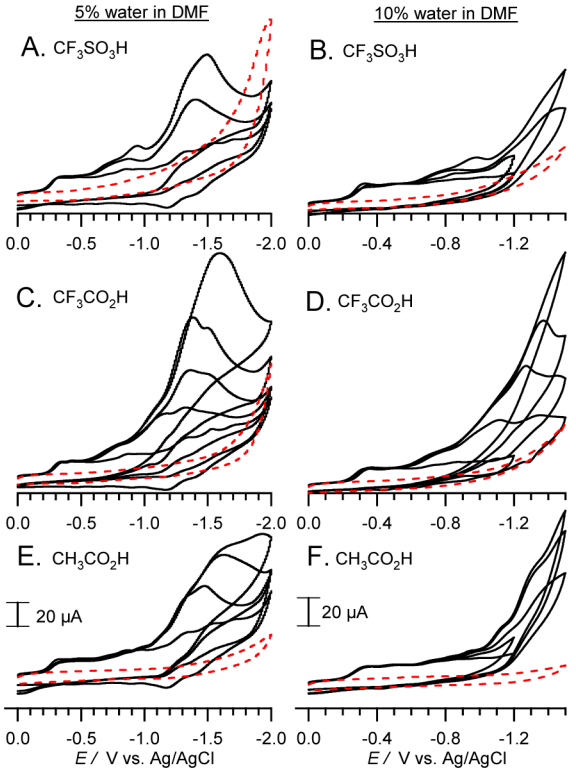

Figure 3. Cyclic voltammograms in DMF/5% H_2O (A, C, E) or DMF/10% H_2O (B, D, F) of 1.0 mM $[\{(Ph_2phen)_2Ru(dpp)\}_2RhBr_2]^{5+}$. (A and B) 0, 5, and 10 equiv of CF_3SO_3H. (C and D) 0, 5, 10, 15, and 25 equiv of CF_3CO_2H. (E and F) 0, 5, 10, and 15 equiv of CH_3CO_2H. CVs in the absence of catalyst are shown for 22 mM acid (dashed red line).

Kinetics of Catalysis. For a reaction that is first order in catalyst and second order in acid, the catalytic current, i_c, is given by eq 1 where n = 2 electrons, F is Faraday's constant, A is the electrode area, D is the diffusion coefficient, and k is the observed rate constant.[86−88] Equation 1 assumes an EC_{cat} mechanism and applies to conditions in which catalysis is pseudozeroth order in substrate; i.e., catalytic current exhibits a plateau. As shown in Figures S1 and S2, plots of catalytic current versus [acid] or [catalyst] are linear. The peak current, i_p, for a reversible one-electron redox couple is given by eq 2 (ν = scan rate in V s^{-1}, R = the ideal gas constant, and T = temperature). The ratio of i_c/i_p in eq 3 provides a convenient method for estimating third order $[H^+]$-dependent rate constants by plotting the slope of i_c/i_p versus [acid] as a function of $\nu^{-1/2}$.[89]

$$i_c = nFA[\mathrm{cat}]\sqrt{Dk[H^+]^2} \quad (1)$$

$$i_p = 0.4463FA[\mathrm{cat}]\sqrt{F\nu D/RT} \quad (2)$$

$$\frac{i_c}{i_p} = \frac{n}{0.4463}\sqrt{\frac{RTk[H^+]^2}{F\nu}} = 0.72\sqrt{\frac{k[H^+]^2}{\nu}} \quad (3)$$

Voltammograms for electrocatalytic acid reduction using **1Br$_2$** did not exhibit pseudozeroth order kinetics in acid (no plateau current) under most conditions. Thus, it was not possible to calculate turnover frequencies at potentials of highest activity using eq 3. For conditions in which catalytic current is independent of $[H^+]$, eq 3 simplifies to i_c/i_p = 0.72

DOI: 10.1021/acs.inorgchem.5b01536
Inorg. Chem. 2015, 54, 8148−8157

Table 1. Summary of CV and Bulk Reduction Data[a]

acid	$E_{HA}°$[b]	E_{cat}[c]	η[d]	faradaic yield,[e] %	turnovers[f]
CF_3SO_3H	−0.21	−0.82	0.61	72 ± 8	95 ± 8
CF_3CO_2H	−0.45	−0.90	0.45	81 ± 8 (100)[g]	100 ± 10 (415)[g]
CH_3CO_2H	−1.0	−1.10	0.10	85 ± 3	116 ± 4

[a]CV experiments were performed using 1.0 mM **1Br$_2$** or **1Cl$_2$** in DMF with 0.1 M Bu_4NPF_6. Bulk electrolysis was performed in duplicate using 55 μM **1Br$_2$** in DMF at an applied potential of −1.4 V vs Ag/AgCl. [b]Standard potential for the reduction of acid in DMF vs Ag/AgCl. [c]Onset of catalytic current. [d]Overpotential in V. [e]Determined using the equation $Q = nFN$ where Q = charge, n = 2, F = 96485 C mol^{-1}, and N = moles of H_2. [f]Moles H_2 per mole catalyst after 2 h. [g]10 h experiment.

$(k/v)^{1/2}$, and the turnover frequency can be calculated from the ratio of i_c/i_p at a given scan rate.[55] This condition was met for reduction of CH_3CO_2H in DMF/10% water in which the turnover frequencies are 4.1 and 3.0 s^{-1} for **1Br$_2$** and **1Cl$_2$**, respectively. It is noted that these values do not reflect the high activity, and are viewed as a lower limit in which the catalysis is saturated in acid.

Bulk Electrolysis. Bulk electrolysis experiments were performed using **1Br$_2$** to confirm H_2 production and Faradaic yields and to access the long-term activity under continuous electrolysis. For comparative experiments between acids, a potential of −1.4 V was applied (Table 1). During 2 h experiments, H_2 was generated with Faradaic yields of 70−85% and turnovers of 80−116. A lower TOF and decrease in H_2 generation using CF_3SO_3H may reflect catalyst decomposition during extended exposure to the strong acid.

Rates of H_2 generation and coulometry were similar for CF_3SO_3H, CF_3CO_2H, and CH_3CO_2H (Figure 4). Similar rates

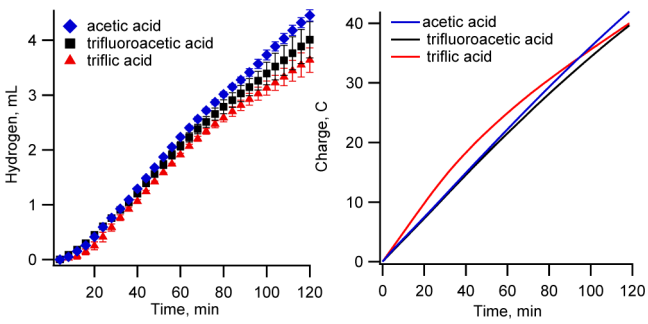

Figure 4. H_2 generation and coulometry for bulk electrolysis experiments using 55 μM $[\{(Ph_2phen)_2Ru(dpp)\}_2RhBr_2]^{5+}$ in DMF with 50 mM acid. The applied potential was −1.4 V vs Ag/AgCl. Experiments are the average of two trials.

of H_2 evolution among acid substrates are supported by voltammetric data. At E_p, the ratio of i_c/i_p is comparable for CF_3SO_3H, CF_3CO_2H, and CH_3CO_2H. Control experiments generate H_2 at −1.4 V with low charge efficiency, and activity ceases after a short time. Catalyst stability was studied during a 10 h experiment after which 16.7 mL of H_2 was produced in quantitative charge yield and 415 catalytic turnovers.

Spectroelectrochemistry During Catalysis. The Ru^{II}−Rh^{III}−Ru^{II} supramolecules are strong visible light absorbers, and color changes accompanying oxidation state changes are clearly visible. During bulk electrolysis experiments, a color change from yellow to purple was observed after acid consumption, coincident with a plateau in H_2 evolution. Catalysis resumed upon addition of acid, and the yellow color reappeared. This process was monitored by spectroelectrochemistry (Figure 5). The absorption spectrum of **1Br$_2$** exhibits transitions at 350, 420, and 515 nm which are assigned as

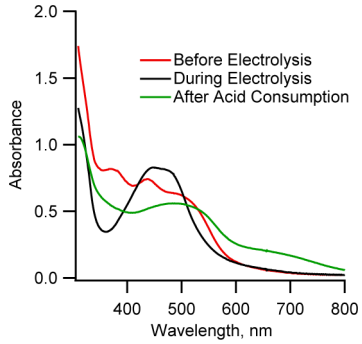

Figure 5. Spectroelectrochemistry during bulk electrolysis of $[\{(Ph_2phen)_2Ru(dpp)\}_2RhBr_2]^{5+}$ in the presence of CF_3CO_2H with an applied potential of −1.4 V vs Ag/AgCl.

intraligand dpp($\pi \rightarrow \pi^*$) transitions, and Ru(dπ) → Ph_2phen(π^*), and Ru(dπ) → dpp(π^*) MLCT transitions, respectively.[25] During electrolysis with CF_3CO_2H, absorptivity decreased at 350 and 520 nm and increased from 420 to 480 nm. After acid consumption, two broad bands at 500 and 680 nm appeared. The final change was reversed by addition of acid, and the process could be repeated multiple times. Reduction at −1.4 V is sufficiently negative to reduce the bridging ligands as indicated by bleaching of the dpp($\pi \rightarrow \pi^*$) and Ru(dπ) → dpp(π^*) transitions. The Ru(dπ) → Ph_2phen(π^*), CT absorptions remain unperturbed in the reduced state since the Ph_2phen ligand is reduced at more negative potentials. After acid consumption at −1.4 V, the molecule is highly reduced with numerous Rh(I)-based (dpp^-)-based absorptions.[90]

After reduction, the purple solution was purged with H_2 for 30 min with no apparent spectroscopic changes. This demonstrates that H_2 does not react with the reduced catalyst to form a Rh(III) dihydride and implies accumulation of H_2 alone should not decrease the activity of hydrogen evolution. Resistance to H_2 addition contrasts with $[Rh(bpy)_2]^+$ which readily adds H_2 to form the Rh(III) dihydride $[Rh^{III}(bpy)_2(H)_2]^+$.[91,92] This experiment does not disprove a Rh(III) dihydride as the active H_2 production species, but it verifies that the equilibrium reaction between such a dihydride and H_2 strongly favors H_2. The spectroscopic changes associated with acid consumption and catalyst regeneration by acid addition provide evidence for homogeneous catalysis and stability of the catalyst in a variety of oxidation states.

Homogeneity and Catalyst Stability. Determining the homogeneous or heterogeneous nature of the catalyst is important for mechanistic considerations.[93] Formation of nanoparticle catalysts from soluble precursors should be considered especially under the reducing or oxidizing conditions of artificial photosynthetic reactions.[94−99] In the electrolysis experiments, a small deviation from linear kinetics toward sigmoidal behavior might hint at heterogeneous

DOI: 10.1021/acs.inorgchem.5b01536
Inorg. Chem. 2015, 54, 8148−8157

catalysis; however, the apparent lag period could also result from slow detection of H_2 in the headspace. Control experiments without catalyst using new carbon cloth electrodes exhibit similar curvature in H_2 detection. The spectroelectrochemistry experiments and the reversible spectral changes associated with catalysis, substrate consumption, and substrate addition are more consistent with homogeneous behavior. To probe this question further, several basic tests were performed. CVs were recorded in pure DMF followed by two consecutive CVs with 15 equiv of acid. A third CV was recorded after carefully polishing the electrode (Figure S5). For CH_3CO_2H and CF_3CO_2H, all CVs in the acidic solution were identical regardless of polishing supporting the molecular and not precipitated identity of the catalyst. In the presence of CF_3SO_3H, slight deviation was observed on the second scan without polishing the electrode. To test for acid-induced absorption or decomposition, a CV was recorded in pure DMF with 1 mM catalyst, and the electrode was transferred to catalyst-free DMF/CF_3CO_2H. Current was slightly greater than background current supporting minor adsorption of the catalyst. To confirm adsorption of the supramolecular catalyst (as opposed to electrodeposition) a polished electrode was soaked in DMF/catalyst for 5 min after which a CV was recorded in pure solvent. Current similar to that of the previous experiment confirms the adsorbed nature of the molecular catalyst to the electrode. Bulk electrolysis experiments employed carbon cloth working electrodes. Identical results were obtained for sequential catalytic experiments with the same electrode and fresh solutions. Control experiments with a previously used or fresh electrode showed the same low activity for H_2 production. These experiments support the notion of molecular catalysis with minor adsorption of these supramolecules being possible under selective conditions. Electrodeposition is disfavored, but formation of dissolved nanoparticles is not ruled out.

Analysis of Reduced Species. Knowledge of active species and intermediates is necessary to formulate a working mechanism for the catalytic reaction. The $[\{(Ph_2phen)_2Ru(dpp)\}_2RhX_2]^{5+}$ supramolecules are inherently difficult to analyze by NMR due to overlapping ^1H resonances and mixtures of coordination isomers. Likewise, absorption spectra characterized by broad transitions provide no definitive identification of species. In contrast, the unique redox units provide an opportunity to analyze Rh^I speciation since the ligand and metal redox potentials are sensitive to coordination environment but insensitive to geometric isomerization.[100,101]

The reductive electrochemistry of $[cis\text{-}Rh^{III}(\alpha\text{-diimine})_2X_2]^+$ complexes is known to proceed via an ECEC mechanism to provide $[Rh^I(\alpha\text{-diimine})_2]^+$.[30,102] Previous work in the Brewer group has assumed identical behavior in supramolecular complexes with a $cis\text{-}Rh^{III}X_2$ catalytic center. In this section we present electrochemical evidence for the intact Ru^{II}–Rh^I–Ru^{II} supramolecule and discuss the effect of solvent and water on product distribution: namely, preferential dissociation of $[(Ph_2phen)_2Ru(dpp)]^{2+}$ when the bound halide is poorly soluble.

The CV of $\mathbf{1Br_2}$ in freshly distilled CH_3CN is shown in Figure 6 before (trace a) and after electrolysis at −0.55 V (trace b). There were 2 equiv of charge consumed during the electrolysis, consistent with reduction from Rh(III) to Rh(I). After electrolysis, the reductive CV showed an irreversible wave at −0.63 V and a reversible couple at −1 V. Oxidative processes were more complicated. Two irreversible waves at 0.74 and

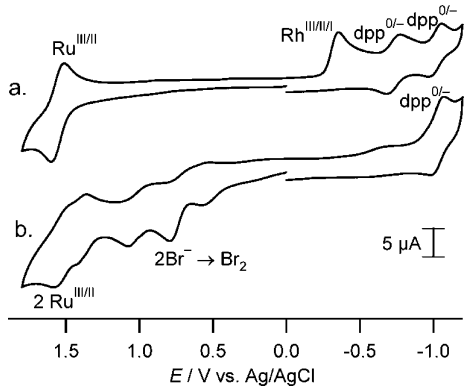

Figure 6. Cyclic voltammograms of $[\{(Ph_2phen)_2Ru(dpp)\}_2RhBr_2]^{5+}$ in CH_3CN prior to reduction (a) and after electrolysis at −0.55 V (b).

1.03 V were followed by two reversible couples at $E_{1/2}$ = 1.54 and 1.38 V. The irreversible waves are oxidation of Br^- to Br_2 confirmed by literature data and by a CV with added Bu_4NBr.[103] The reversible couples at 1.54 and 1.38 V suggest $Ru^{III/II}$ processes: the wave at 1.54 V remained unchanged from $\mathbf{1Br_2}$ while the couple at 1.38 V is identical to the $Ru^{III/II}$ couple of $[(Ph_2phen)_2Ru(dpp)]^{2+}$ in CH_3CN (the couple at −1 V is also identical to the first reduction of this species).[25] The presence of $[(Ph_2phen)_2Ru(dpp)]^{2+}$ *and* Br^- after reduction in dry CH_3CN is evidence for a mixture of electrogenerated Rh(I) species in dry CH_3CN: the expected $[\{(Ph_2phen)_2Ru(dpp)\}_2Rh^I]^{5+}$ and $[(Ph_2phen)_2Ru(dpp)Rh^IBr_2]^+$ in contrast to the reported and widely assumed halide loss for $[Rh^I(\alpha\text{-diimine})_2]^+$ complexes.[23−27,30,102]

Electrochemical reduction and CV analysis was repeated for $\mathbf{1Cl_2}$ (Figure 7). In dry CH_3CN, redox processes (trace a) are similar to $\mathbf{1Br_2}$. After $2e^-$ reduction at −0.55 V, a limited amount of Cl^- was detected in solution as indicated by the small $2Cl^-/Cl_2$ couple at 1.04 V (b). Two reversible oxidations were observed at 1.54 and 1.38 V and an irreversible reduction appeared at −0.63 followed by a reversible couple at −1.0 V. The experiment was repeated with 1 M H_2O in CH_3CN (traces c and d), and little Cl^- was observed after reduction. Further electrolysis at −0.85 V, consumed $1e^-$ and the product CV (e) showed appreciable current for Cl^- oxidation. With 3 M H_2O in CH_3CN (f and g) Cl^- was detected after $2e^-$ reduction.

Bulk reduction and CV analysis in CH_3CN reveal varied product distribution with dependence on halide. For $\mathbf{1Br_2}$, Br^- was detected upon reduction in dry CH_3CN, whereas 3 M H_2O was necessary to observe Cl^- dissociation after reduction of $\mathbf{1Cl_2}$. Loss of X^- implies formation of the intact supramolecule $[\{(Ph_2phen)_2Ru(dpp)\}_2Rh^I]^{5+}$. When Cl^- does not dissociate after reduction, $[(Ph_2phen)_2Ru(dpp)Rh^ICl_2]^+$ and $[(Ph_2phen)_2Ru(dpp)]^{2+}$ are formed selectively. The appearance of Cl^- after electrolysis at −0.85 V allows assignment of the irreversible couple at −0.63 V as the $dpp^{0/-}$ couple in the Ru^{II}–Rh^I species (Figure 7d), which triggers dissociative decomposition upon reduction. Scheme 1 summarizes the product dependence on solvent and anion.

The simplest interpretation for Br^- but not Cl^- dissociation upon $2e^-$ reduction in dry CH_3CN is poor solvation of the chloride ion in acetonitrile. The solubilities of KCl and KBr in CH_3CN were reported as 8×10^{-5} and 1.6×10^{-3} molal, respectively, and small amounts of water greatly increased solubility.[104] The two-electron reduction of $\mathbf{1Cl_2}$ triggers dissociation of one $[(Ph_2phen)_2Ru(dpp)]^{2+}$ moiety which is

DOI: 10.1021/acs.inorgchem.5b01536
Inorg. Chem. 2015, 54, 8148−8157

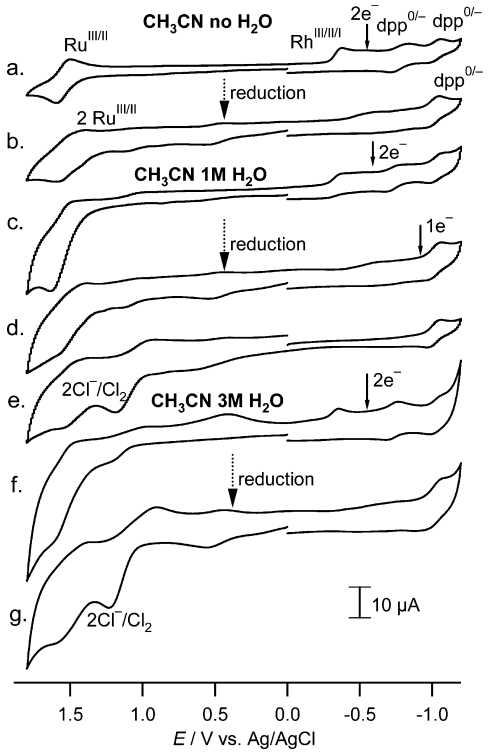

Figure 7. Cyclic voltammograms of $[\{(Ph_2phen)_2Ru(dpp)\}_2RhCl_2]^{5+}$ in CH_3CN (a), after $2e^-$ reduction at −0.55 V (b), in 1 M water/CH_3CN (c) after $2e^-$ reduction in 1 M water at −0.55 V (d) or $3e^-$ reduction at −0.85 V (e). In traces f and g, the experiment was repeated with 3 M water and $2e^-$ reduction at −0.55 V.

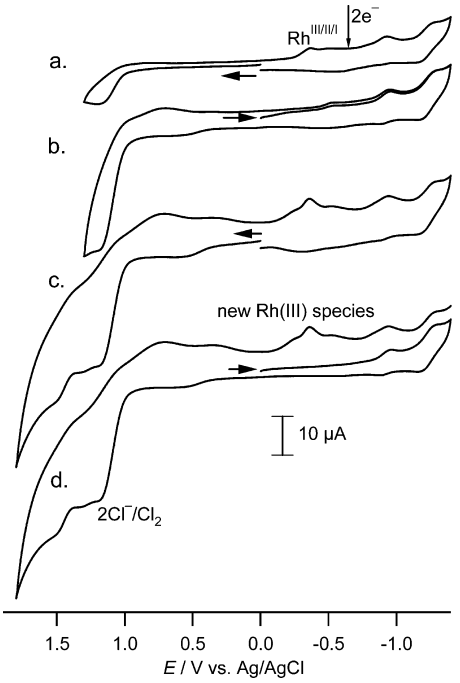

Figure 8. Cyclic voltammograms of $[\{(Ph_2phen)_2Ru(dpp)\}_2RhCl_2]^{5+}$ in DMF (a) and after controlled potential electrolysis at −0.55 V scanning sweeping through +1.3 V (b) or +1.8 V (c and d). Arrows indicate direction of initial scan.

highly soluble in CH_3CN, and two Cl^- ligands are retained by Rh(I) unless water is added to solvate the Cl−.

Reduction and product analysis were repeated in DMF with significantly different outcomes compared to those in CH_3CN. Figure 8 shows the CV of **1Cl$_2$** (a) and after reduction (b). The absence of the $Rh^{III/II/I}$ wave confirmed $2e^-$ reduction, and oxidation of Cl^- was observed at +1 V demonstrating labilization of the Cl^- in DMF. A CV obtained by sweeping the same solution through +1.8 V (c) provided a new irreversible reduction at E_p^c = −0.34 V. This wave was not apparent when scanning first reductively (d) or sweeping only through +1.3 V (b). **1Br$_2$** displayed identical behavior with the exception that oxidation through 1.3 V was sufficient to generate a new reduction wave at −0.51 V (Supporting Information Figure S6). The $Ru^{III/II}$ couple appeared near 1.5 V.

Observation of Cl^- or Br^- in solution after reduction of $[\{(Ph_2phen)_2Ru(dpp)\}_2RhX_2]^{5+}$ in DMF demonstrates facile halide dissociation from Rh(I). The solubilities of KCl and KBr in DMF are reported as 2.44×10^{-3} and 7.6×10^{-2} molal, respectively.[104] The major Rh(I) species should be $[\{(Ph_2phen)_2Ru(dpp)\}_2Rh^I]^{5+}$. The presence of this species and its stability are supported by irreversible redox waves at −0.34 and −0.51 V after anodic sweeps of the Cl^- and Br^- containing solutions. These potentials are comparable to the $Rh^{III/II/I}$ reduction of the starting materials and are assigned as Rh-based reductions of $[\{(Ph_2phen)_2Ru(dpp)\}_2RhL_2]^{n+}$ complexes where L = X^- and/or solvent. Different potentials depending on the presence of Cl^- or Br^- support recoordination of at least one anion when Rh(I) is reoxidized.

Scheme 1. Solvent-Dependent Speciation upon Two-Electron Reduction of $[\{(Ph_2phen)_2Ru(dpp)\}_2RhX_2]^{5+}$ Complexes

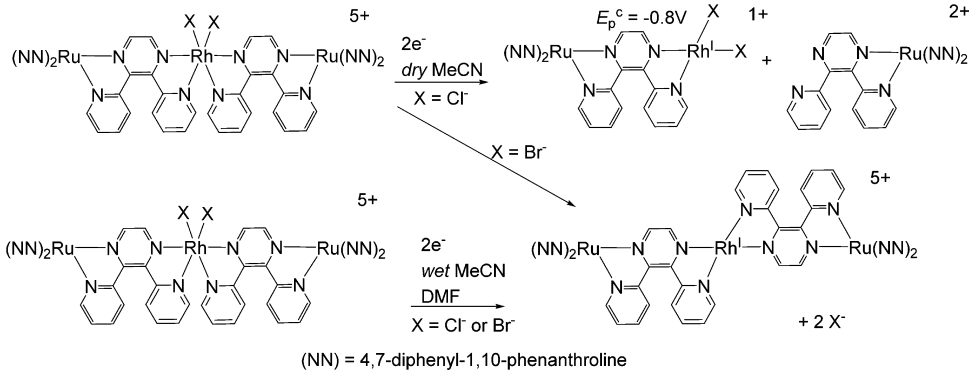

(NN) = 4,7-diphenyl-1,10-phenanthroline

DOI: 10.1021/acs.inorgchem.5b01536
Inorg. Chem. 2015, 54, 8148−8157

DISCUSSION

Results in this work demonstrate the applicability of supramolecular complexes $[\{(Ph_2phen)_2Ru(dpp)\}_2RhX_2]^{5+}$ as electrocatalysts for proton reduction. Although catalysis using the complicated supramolecule instead of the simpler $[RhX_2(dpp)_2]^+$ core may appear counterintuitive, we propose surface-confined photoelectrocatalysis as a future research direction in which the applied potential can be alleviated if solar energy is directly utilized by the appended Ru(II) chromophore. Furthermore, the exact potentials of redox couples of interest are different when the dpp ligands bridge Rh centers. This is shown in Figure 2D in which reduction of Rh(III) in the trimetallics is more facile than that for $[RhCl_2(dpp)_2]^+$.

Kinetic analysis of the CVs is difficult owing to multiple underlying redox couples of $[\{(Ph_2phen)_2Ru(dpp)\}_2RhX_2]^{5+}$ within the electrocatalytic response. Analysis according to an EC_{cat} mechanism is an oversimplification since each successive reduction leads to a new species which may increase (or decrease) the rate of catalysis. Under most conditions, the CVs do not exhibit the canonical S-shaped plateau response typical of systems in which an EC_{cat} simplification is appropriate. The absence of plateau current may result from substrate consumption; however, the catalytic response may be perturbed by other phenomena including catalyst decomposition or inhibition by product. The foot-of-the-wave analysis avoids complications in the low potential region by considering only the initial CV catalytic response.[105] For $[\{(Ph_2phen)_2Ru(dpp)\}_2RhX_2]^{5+}$, this method is not appropriate because the specific redox couple which triggers catalysis is unknown, further reductions generate new species, and a large deviation from ideal behavior is observed.

Despite the complications of kinetic analysis, experiments with acids of varied strength provide insight into important redox couples and plausible intermediates. Catalyst activation proceeds through $2e^-$ reduction of the *cis*-$Rh^{III}X_2$ precatalysts via an ECEC mechanism in DMF eqs i–iv.[30] This reaction was verified by bulk electrolysis and CV analysis. The $[(Ph_2phen)_2Ru]^{2+}$ units are omitted from the following equations for clarity.

$$[(dpp)Rh^{III}Br_2(dpp)]^{5+} + e^- \rightarrow [(dpp)Rh^{II}Br_2(dpp)]^{4+} \quad \text{(i)}$$

$$[(dpp)Rh^{II}Br_2(dpp)]^{4+} \rightarrow [(dpp)Rh^{II}Br(dpp)]^{5+} + Br^- \quad \text{(ii)}$$

$$[(dpp)Rh^{II}Br(dpp)]^{5+} + e^- \rightarrow [(dpp)Rh^{I}Br(dpp)]^{4+} \quad \text{(iii)}$$

$$[(dpp)Rh^{I}Br(dpp)]^{4+} \rightarrow [(dpp)Rh^{I}(dpp)]^{5+} + Br^- \quad \text{(iv)}$$

The $[(dpp)Rh^{I}(dpp)]^{5+}$ should be strongly basic considering the pK_a values of related Rh(III) hydrides in H_2O, i.e., $[Rh^{III}(bpy)_2(H)(H_2O)]^{2+}$ (9.5), $[Rh^{III}(NH_4)_2(H)(H_2O)]^{2+}$ (>14), and $[Rh^{III}(dmgH)_2(H)(PPh_3)]$.[106] Protonation by CF_3CO_2H and CF_3SO_3H (eq v) provides the Rh(III)–H whereas the reaction with acetic acid ($pK_a \sim 13.2$–13.5)[81,107] perhaps favors the reverse equilibrium. The Rh(III)–H is most likely octahedral with solvent or A^- as the sixth ligand.

$$[(dpp)Rh^{I}(dpp)]^{5+} + HA \rightleftarrows [(dpp)Rh^{III}(H)(dpp)]^{6+} + A^- \quad \text{(v)}$$

In Figure 2, there is no catalysis at the $Rh^{III/II/I}$ couple. Therefore, reduction of putative Rh(III) hydrides must occur cathodic of the *cis*-$Rh^{III}X_2$ potential. Figure 2A,B shows new reduction couples (peak 5) at −0.75 and −0.62 V. Peak 5 does not trigger catalysis, and its nature is proposed as reduction of $Rh^{III}(H)$ to $Rh^{II}(H)$, eq vi. Consistent with $[Rh(Me_2bpy)_2(H)Cl]^+$, this couple appears ca. 400 mV more negative than the *cis*-$Rh^{III}X_2$ potential.[71] The $Rh(H)^{III/II}$ couple was observed for $[Rh(H)(TPP)]$ at −1.3 V versus Ag/AgCl,[77] at −1.33 V for $[Rh(Me_5C_5)(L)(H)]^+$ (L = substituted bipyridine) in water,[108] and at −1.34 V for $[Rh(Me_5C_5)(bpy)(H)]^+$ in CH_3CN.[109] The anodic shift for this reduction in the present work is attributed to the weak σ-donor and strong π-acceptor properties of the dpp bridging ligands which render Rh electron deficient and easily reduced. Slight differences in the potential for eq vi in the presence of CF_3CO_2H or CF_3SO_3H support conjugate base coordination to the $Rh^{III}(H)$ species; however, this notation is omitted for consistency in the equations.

$$[(dpp)Rh^{III}(H)(dpp)]^{6+} + e^- \rightarrow [(dpp)Rh^{II}(H)(dpp)]^{5+} \quad \text{(vi)}$$

In stark contrast to the protonolysis of $[Rh^{II}(Me_2bpy)_2(H)]^+$, which reacts with formic acid, or the behavior of related group 9 cobaloxime catalysts,[31,71,110–114] here catalysis is not observed at the proposed $Rh(H)^{III/II}$ couple. No catalysis at the $Rh(H)^{III/II}$ couple shows slow or negligible protonolysis of the $Rh^{II}(H)$ (eq vii) and is likely attributed to the anodic shift (and therefore weaker hydricity) of this couple relative to monometallic Rh complexes.

$$[(dpp)Rh^{II}(H)(dpp)]^{5+} + H^+ \rightarrow [(dpp)Rh^{II}(dpp)]^{6+} + H_2 \quad \text{(vii)}$$

An electrocatalytic wave is triggered near the first $dpp^{0/-}$ couple in the presence of CF_3CO_2H or CF_3SO_3H. Using CF_3CO_2H, the slopes of the voltammogram increase at the second $dpp^{0/-}$ couple. On the basis of this observation, eqs viii and ix are formulated in which the Rh(II) hydride becomes increasingly hydridic and prone to protonolysis as the adjacent ligands are reduced. The product of eq ix is written as Rh(I),dpp(0) since the protonolysis reaction must not necessarily happen within the diffusion layer.

$$[(dpp)Rh^{II}(H)(dpp)]^{5+} + e^- \rightarrow [(dpp)Rh^{II}(H)(dpp^-)]^{4+} \quad \text{(viii)}$$

$$[(dpp)Rh^{II}(H)(dpp^-)]^{4+} + H^+ \rightarrow [(dpp)Rh^{I}(dpp)]^{5+} + H_2 \quad \text{(ix)}$$

The preceding discussion omitted analysis of CH_3CO_2H since reduction of this weaker acid was not observed until −1.05 V. On the basis of the range of possible pK_a values for Rh(III) hydrides, the Rh(I) is unlikely to be protonated by acetic acid until one or more dpp ligands are reduced, thereby generating a more basic Rh(I) center. At the more negative potentials, eqs viii and ix apply.

The proximity of electrocatalysis to the $dpp^{0/-}$ couple(s) has an interesting mechanistic implication; namely, reduction of dpp is possible through reductive quenching of the Ru(II) excited state. Photocatalytic experiments have shown catalysis is initiated by reductive quenching of the ^{3}MLCT state followed by thermal electron transfer from dpp^- to $Rh^{III}X_2$.[115] The present data reveals that ligand-based reductions increase the

DOI: 10.1021/acs.inorgchem.5b01536
Inorg. Chem. 2015, 54, 8148–8157

basicity of Rh(I) (i.e., the reaction of Rh(I) with CH_3CO_2H) and increase the rate or proton attack on putative Rh(II) hydride intermediates. Although photocatalytic experiments were performed in basic conditions (CH_3CN or DMF, H_2O, *N*,*N*-dimethylaniline pH ∼ 9), protonation of the Rh(I) species is feasible considering that the pK_a for $[Rh^{III}(bpy)_2(H)(H_2O)]^{2+}$ is 9.5 in water.[106]

A consistent trend in photocatalysis has been higher efficiency for Rh(III) dibromide precursors compared to Rh(III) dichloride complexes. Furthermore, catalysis is more efficient in DMF versus acetonitrile.[25,78] A number of explanations have been proposed including inhibition through coordination of CH_3CN to Rh, and a greater driving force for Rh(I) formation in the *cis*-$RhBr_2$ complexes due to a slightly more anodic $Rh^{III/II/I}$ couple. The latter hypothesis should only apply if halide remains active in the catalytic cycle. In the present work, we have analyzed the Rh(I) species formed upon $2e^-$ reduction in DMF and CH_3CN. Data suggest a Ru^{II}−Rh^{I}−Ru^{II} trimetallic species is exclusively formed in DMF, whereas reduction in acetonitrile generates a mixture of the trimetallic and $[(Ph_2phen)Ru(dpp)]^{2+}$. The $\mathbf{1Cl_2}$ yields a reduced trimetallic in CH_3CN only with >3 M H_2O suggesting the solubility of the anion controls the concentrations of the active catalyst. These studies present a cautionary warning for analysis of supramolecular devices for AP. Properties expected of model compounds may not hold true for complicated photo- and electroactive supramolecular structures of large size and high charge.

CONCLUSIONS

The supramolecular complexes $[\{(Ph_2phen)_2Ru(dpp)\}_2RhX_2]^{5+}$ with X = Cl^- and Br^- function as electrocatalysts for the production of H_2 from acids in DMF and DMF/water mixtures. This provides impetus for the design of supramolecular photoelectrocatalysts which combine light and electrochemical energy to reduce the overpotential for production of H_2 from water. Surface confinement may also influence redox couples in these systems. Voltammetry experiments with varied acids suggest protonation of a ligand-reduced $[(dpp)Rh^{II}(H)(dpp^-)]^{4+}$ species as a key step in catalysis. In the presence of weak acids, the Rh(I) is not protonated until after a ligand-based reduction. The important $Rh(H)^{III/II}$ couple is estimated as −0.75 V; therefore, the Rh(II) hydride can be generated photochemically through reductive quenching of the Ru(II)* excited state followed by ground state electron transfer. Analysis of reduction products provided insight into the influence of solvent on product distribution. The solubility of the X^- is an important consideration for generating the intact reduced photocatalyst. Studies regarding surface immobilization and catalysis in pure water are now underway.

EXPERIMENTAL SECTION

The $[\{(Ph_2phen)_2Ru(dpp)\}_2RhX_2](PF_6)_5$ catalysts were prepared by a published procedure and purified by chromatography on Sephadex LH-20.[25] $RuCl_3{\cdot}nH_2O$, $RhBr_3{\cdot}nH_2O$, and Ph_2phen were purchased from Alfa Aesar. DMF was high purity Burdick & Jackson grade. Bu_4NBr was purchased from Acros Organics. CF_3SO_3H, CF_3CO_2H, and dpp were purchased from Aldrich. Glacial acetic acid was purchased from Crescent Chemical Co. Bu_4NPF_6 was prepared by the metathesis reaction of Bu_4NBr and HPF_6, crystallized thrice from ethanol, and dried at 100 °C.

Cyclic voltammograms were recorded using a standard three-electrode cell controlled by a Bioanalytical System (BAS) Epsilon potentiostat. The working electrode was a glassy carbon disk, and the counter electrode was a Pt wire. The reference electrode was a Ag wire in a glass tube equipped with a porous Vycor tip and filled with 3 M KCl (aq). This electrode was calibrated against the $Fc^{+/0}$ couple in DMF at −0.56 V. Bu_4NPF_6 (0.1 M) was used as the supporting electrolyte. Samples were purged with Ar prior to scans and blanketed with Ar during CVs. Aliquots of acid (0.1 M) were added to 1 mL portions of solutions of 1.0 mM $[\{(Ph_2phen)_2Ru(dpp)\}_2RhX_2](PF_6)_5$ in DMF or DMF/water mixtures. The working electrode was polished between successive CVs. To determine the reaction order with respect to catalyst, a 1 mL solution of 24 mM CF_3CO_2H and 100 mM $TBAPF_6$ was titrated with a stock solution of 20 mM $[\{(Ph_2phen)_2Ru(dpp)\}_2RhBr_2](PF_6)_5$ containing 24 mM CF_3CO_2H and 100 mM electrolyte.

Bulk reduction experiments were performed using a custom-built airtight two-compartment cell equipped with a threaded joint for attachment of a HY-OPTIMA 700 in-line process solid state hydrogen sensor from H_2scan for real-time monitoring of of H_2 produced. A Pt mesh auxiliary electrode was separated from the catalyst solution by a medium porosity frit. The working electrode was a carbon cloth attached to a copper wire using an alligator clip. For all experiments, both chambers were deoxygenated with argon at equal pressures. Appropriate solutions were deoxygenated separately by purging with Ar, and then 28 mL was injected simultaneously into each chamber via syringe. During the injection, pressure was vented through a bubbler. The HY-OPTIMA sensor was calibrated by injecting known amounts of H_2 gas into the working electrode chamber containing 28 mL of solution. Under these conditions, transfer of solution through the frit to the auxiliary chamber did not occur until the hydrogen content in the headspace reached ∼10−12% or ca. 3 mL. For a 10 h experiment, the working compartment was purged with Ar after accumulating 10−12% hydrogen in the headspace.

ASSOCIATED CONTENT

Supporting Information

The Supporting Information is available free of charge on the ACS Publications website at DOI: 10.1021/acs.inorgchem.5b01536.

Plots of catalytic current versus [acid] and [catalyst]; CVs for electrocatalytic reduction of CF_3CO_2H, CF_3SO_3H, and CH_3CO_2H using $[\{(Ph_2phen)_2Ru(dpp)\}_2RhCl_2](PF_6)_5$; CVs comparing $[\{(Ph_2phen)_2Ru(dpp)\}_2RhCl_2](PF_6)_5$ and $[RhCl_2(dpp)_2]^+$; CVs showing effect of polishing the electrode on catalytic response, and $2e^-$ reduction of $[\{(Ph_2phen)_2Ru(dpp)\}_2RhBr_2](PF_6)_5$ in DMF (PDF)

AUTHOR INFORMATION

Corresponding Author

*E-mail: gmanbeck@bnl.gov.

Present Address

†Department of Chemistry, Brookhaven National Laboratory, Upton, NY 11973.

Author Contributions

The manuscript was written through contributions of all authors. All authors have given approval to the final version of the manuscript.

Notes

The authors declare no competing financial interest.

‡Deceased October 24, 2014.

ACKNOWLEDGMENTS

This material is based upon work supported by the Department of Energy under award number DE-FG02-05ER15751. The

DOI: 10.1021/acs.inorgchem.5b01536
Inorg. Chem. 2015, 54, 8148−8157

authors would like to thank Dr. Etsuko Fujita for helpful comments during the preparation of this manuscript.

REFERENCES

(1) Andreiadis, E. S.; Chavarot-Kerlidou, M.; Fontecave, M.; Artero, V. *Photochem. Photobiol.* **2011**, *87*, 946−964.
(2) Tinker, L. L.; McDaniel, N. D.; Bernhard, S. *J. Mater. Chem.* **2009**, *19*, 3328−3337.
(3) Gust, D.; Moore, T. A.; Moore, A. L. *Acc. Chem. Res.* **2009**, *42*, 1890−1898.
(4) Song, W.; Chen, Z.; Brennaman, M. K.; Concepcion, J. J.; Patrocinio, A. O. T.; Iha, N. Y. M.; Meyer, T. J. *Pure Appl. Chem.* **2011**, *83*, 749−768.
(5) Alstrum-Acevedo, J. H.; Brennaman, M. K.; Meyer, T. J. *Inorg. Chem.* **2005**, *44*, 6802−6827.
(6) McDaniel, N. D.; Bernhard, S. *Dalton Trans.* **2010**, *39*, 10021−10030.
(7) Probst, B.; Guttentag, M.; Rodenberg, A.; Hamm, P.; Alberto, R. *Inorg. Chem.* **2011**, *50*, 3404−3412.
(8) Wang, X. H.; Goeb, S.; Ji, Z. Q.; Pogulaichenko, N. A.; Castellano, F. N. *Inorg. Chem.* **2011**, *50*, 705−707.
(9) Fukuzumi, S.; Kobayashi, T.; Suenobu, T. *Angew. Chem., Int. Ed.* **2011**, *50*, 728−731.
(10) Cline, E. D.; Adamson, S. E.; Bernhard, S. *Inorg. Chem.* **2008**, *47*, 10378−10388.
(11) McCormick, T. M.; Calitree, B. D.; Orchard, A.; Kraut, N. D.; Bright, F. V.; Detty, M. R.; Eisenberg, R. *J. Am. Chem. Soc.* **2010**, *132*, 15480−15483.
(12) Streich, D.; Astuti, Y.; Orlandi, M.; Schwartz, L.; Lomoth, R.; Hammarstrom, L.; Ott, S. *Chem. - Eur. J.* **2010**, *16*, 60−63.
(13) Pellegrin, Y.; Odobel, F. *Coord. Chem. Rev.* **2011**, *255*, 2578−2593.
(14) Fihri, A.; Artero, V.; Razavet, M.; Baffert, C.; Leibl, W.; Fontecave, M. *Angew. Chem., Int. Ed.* **2008**, *47*, 564−567.
(15) Mulfort, K. L.; Tiede, D. M. *J. Phys. Chem. B* **2010**, *114*, 14572−14581.
(16) Utschig, L. M.; Silver, S. C.; Mulfort, K. L.; Tiede, D. M. *J. Am. Chem. Soc.* **2011**, *133*, 16334−16337.
(17) Knoll, J. D.; Arachchige, S. M.; Brewer, K. J. *ChemSusChem* **2011**, *4*, 252−261.
(18) Ozawa, H.; Kobayashi, M.; Balan, B.; Masaoka, S.; Sakai, K. *Chem. - Asian J.* **2010**, *5*, 1860−1869.
(19) Jasimuddin, S.; Yamada, T.; Fukuju, K.; Otsuki, J.; Sakai, K. *Chem. Commun.* **2010**, *46*, 8466−8468.
(20) Rau, S.; Schaefer, B.; Gleich, D.; Anders, E.; Rudolph, M.; Friedrich, M.; Goerls, H.; Henry, W.; Vos, J. G. *Angew. Chem., Int. Ed.* **2006**, *45*, 6215−6218.
(21) Peuntinger, K.; Pilz, T. D.; Staehle, R.; Schaub, M.; Kaufhold, S.; Petermann, L.; Wunderlin, M.; Gorls, H.; Heinemann, F. W.; Li, J.; Drewello, T.; Vos, J. G.; Guldi, D. M.; Rau, S. *Dalton Trans.* **2014**, *43*, 13683−13695.
(22) Zhang, P.; Wang, M.; Li, C. X.; Li, X. Q.; Dong, J. F.; Sun, L. C. *Chem. Commun.* **2010**, *46*, 8806−8808.
(23) Arachchige, S. A.; Brown, J.; Brewer, K. J. *J. Photochem. Photobiol., A* **2008**, *197*, 13−17.
(24) White, T. A.; Rangan, K.; Brewer, K. J. *J. Photochem. Photobiol., A* **2010**, *209*, 203−209.
(25) White, T. A.; Higgins, S. L. H.; Arachchige, S. M.; Brewer, K. J. *Angew. Chem., Int. Ed.* **2011**, *50*, 12209−12213.
(26) White, T. A.; Whitaker, B. N.; Brewer, K. J. *J. Am. Chem. Soc.* **2011**, *133*, 15332−15334.
(27) Stoll, T.; Gennari, M.; Fortage, J.; Castillo, C. E.; Rebarz, M.; Sliwa, M.; Poizat, O.; Odobel, F.; Deronzier, A.; Collomb, M. N. *Angew. Chem., Int. Ed.* **2014**, *53*, 1654−1658.
(28) Manbeck, G. F.; Brewer, K. J. *Coord. Chem. Rev.* **2013**, *257*, 1660−1675.
(29) Stoll, T.; Castillo, C. E.; Kayanuma, M.; Sandroni, M.; Daniel, C.; Odobel, F.; Fortage, J.; Collomb, M. N. *Coord. Chem. Rev.* **2015**, DOI: 10.1016/j.ccr.2015.02.002.
(30) Kew, G.; DeArmond, K.; Hanck, K. *J. Phys. Chem.* **1974**, *78*, 727−734.
(31) Kayanuma, M.; Stoll, T.; Daniel, C.; Odobel, F.; Fortage, J.; Deronzier, A.; Collomb, M. N. *Phys. Chem. Chem. Phys.* **2015**, *17*, 10497−10509.
(32) Solis, B. H.; Hammes-Schiffer, S. *J. Am. Chem. Soc.* **2011**, *133*, 19036−19039.
(33) Artero, V.; Chavarot-Kerlidou, M.; Fontecave, M. *Angew. Chem., Int. Ed.* **2011**, *50*, 7238−7266.
(34) Losse, S.; Vos, J. G.; Rau, S. *Coord. Chem. Rev.* **2010**, *254*, 2492−2504.
(35) Jacques, P.-A.; Artero, V.; Pecaut, J.; Fontecave, M. *Proc. Natl. Acad. Sci. U. S. A.* **2009**, *106*, 20627−20632.
(36) Hu, X. L.; Brunschwig, B. S.; Peters, J. C. *J. Am. Chem. Soc.* **2007**, *129*, 8988−8998.
(37) Baffert, C.; Artero, V.; Fontecave, M. *Inorg. Chem.* **2007**, *46*, 1817−1824.
(38) Dempsey, J. L.; Brunschwig, B. S.; Winkler, J. R.; Gray, H. B. *Acc. Chem. Res.* **2009**, *42*, 1995−2004.
(39) Capon, J. F.; Ezzaher, S.; Gloaguen, F.; Petillon, F. Y.; Schollhammer, P.; Talarmin, J. *Chem. - Eur. J.* **2008**, *14*, 1954−1964.
(40) Barton, B. E.; Olsen, M. T.; Rauchfuss, T. B. *Curr. Opin. Biotechnol.* **2010**, *21*, 292−297.
(41) Gloaguen, F.; Rauchfuss, T. B. *Chem. Soc. Rev.* **2009**, *38*, 100−108.
(42) Felton, G. A. N.; Mebi, C. A.; Petro, B. J.; Vannucci, A. K.; Evans, D. H.; Glass, R. S.; Lichtenberger, D. L. *J. Organomet. Chem.* **2009**, *694*, 2681−2699.
(43) Ott, S.; Kritikos, M.; Akermark, B.; Sun, L. C.; Lomoth, R. *Angew. Chem., Int. Ed.* **2004**, *43*, 1006−1009.
(44) Evans, D. J.; Pickett, C. J. *Chem. Soc. Rev.* **2003**, *32*, 268−275.
(45) Reisner, E. *Eur. J. Inorg. Chem.* **2011**, *2011*, 1005−1016.
(46) Quentel, F.; Passard, G.; Gloaguen, F. *Energy Environ. Sci.* **2012**, *5*, 7757−7761.
(47) Wang, M.; Chen, L.; Sun, L. C. *Energy Environ. Sci.* **2012**, *5*, 6763−6778.
(48) Stubbert, B. D.; Peters, J. C.; Gray, H. B. *J. Am. Chem. Soc.* **2011**, *133*, 18070−18073.
(49) Bigi, J. P.; Hanna, T. E.; Harman, W. H.; Chang, A.; Chang, C. J. *Chem. Commun.* **2010**, *46*, 958−960.
(50) McNamara, W. R.; Han, Z.; Alperin, P. J.; Brennessel, W. W.; Holland, P. L.; Eisenberg, R. *J. Am. Chem. Soc.* **2011**, *133*, 15368−15371.
(51) Lee, C. H.; Dogutan, D. K.; Nocera, D. G. *J. Am. Chem. Soc.* **2011**, *133*, 8775−8777.
(52) McCrory, C. C. L.; Uyeda, C.; Peters, J. C. *J. Am. Chem. Soc.* **2012**, *134*, 3164−3170.
(53) Singh, W. M.; Baine, T.; Kudo, S.; Tian, S. L.; Ma, X. A. N.; Zhou, H. Y.; DeYonker, N. J.; Pham, T. C.; Bollinger, J. C.; Baker, D. L.; Yan, B.; Webster, C. E.; Zhao, X. *Angew. Chem., Int. Ed.* **2012**, *51*, 5941−5944.
(54) Kilgore, U. J.; Stewart, M. P.; Helm, M. L.; Dougherty, W. G.; Kassel, W. S.; DuBois, M. R.; DuBois, D. L.; Bullock, R. M. *Inorg. Chem.* **2011**, *50*, 10908−10918.
(55) Kilgore, U. J.; Roberts, J. A. S.; Pool, D. H.; Appel, A. M.; Stewart, M. P.; DuBois, M. R.; Dougherty, W. G.; Kassel, W. S.; Bullock, R. M.; DuBois, D. L. *J. Am. Chem. Soc.* **2011**, *133*, 5861−5872.
(56) Helm, M. L.; Stewart, M. P.; Bullock, R. M.; DuBois, M. R.; DuBois, D. L. *Science* **2011**, *333*, 863−866.
(57) Yang, J. Y.; Chen, S.; Dougherty, W. G.; Kassel, W. S.; Bullock, R. M.; DuBois, D. L.; Raugei, S.; Rousseau, R.; Dupuis, M.; DuBois, M. R. *Chem. Commun.* **2010**, *46*, 8618−8620.
(58) Rose, M. J.; Gray, H. B.; Winkler, J. R. *J. Am. Chem. Soc.* **2012**, *134*, 8310−8313.
(59) Andrieux, C. P.; Blocman, C.; Dumasbouchiat, J. M.; Mhalla, F.; Saveant, J. M. *J. Electroanal. Chem. Interfacial Electrochem.* **1980**, *113*, 19−40.

DOI: 10.1021/acs.inorgchem.5b01536
Inorg. Chem. 2015, 54, 8148−8157

(60) Andreiadis, E. S.; Jacques, P. A.; Tran, P. D.; Leyris, A.; Chavarot-Kerlidou, M.; Jousselme, B.; Matheron, M.; Pecaut, J.; Palacin, S.; Fontecave, M.; Artero, V. *Nat. Chem.* **2013**, *5*, 48−53.
(61) Le Goff, A.; Artero, V.; Jousselme, B.; Tran, P. D.; Guillet, N.; Metaye, R.; Fihri, A.; Palacin, S.; Fontecave, M. *Science* **2009**, *326*, 1384−1387.
(62) Tran, P. D.; Le Goff, A.; Heidkamp, J.; Jousselme, B.; Guillet, N.; Palacin, S.; Dau, H.; Fontecave, M.; Artero, V. *Angew. Chem., Int. Ed.* **2011**, *50*, 1371−1374.
(63) Berben, L. A.; Peters, J. C. *Chem. Commun.* **2010**, *46*, 398−400.
(64) Muresan, N. M.; Willkomm, J.; Mersch, D.; Vaynzof, Y.; Reisner, E. *Angew. Chem., Int. Ed.* **2012**, *51*, 12749−12753.
(65) Krawicz, A.; Yang, J. H.; Anzenberg, E.; Yano, J.; Sharp, I. D.; Moore, G. F. *J. Am. Chem. Soc.* **2013**, *135*, 11861−11868.
(66) Kumar, B.; Smieja, J. M.; Kubiak, C. P. *J. Phys. Chem. C* **2010**, *114*, 14220−14223.
(67) Sato, S.; Morikawa, T.; Saeki, S.; Kajino, T.; Motohiro, T. *Angew. Chem., Int. Ed.* **2010**, *49*, 5101−5105.
(68) Ji, Z. Q.; He, M. F.; Huang, Z. J.; Ozkan, U.; Wu, Y. Y. *J. Am. Chem. Soc.* **2013**, *135*, 11696−11699.
(69) Tong, L.; Iwase, A.; Nattestad, A.; Bach, U.; Weidelener, M.; Gotz, G.; Mishra, A.; Bauerle, P.; Amal, R.; Wallace, G. G.; Mozer, A. J. *Energy Environ. Sci.* **2012**, *5*, 9472−9475.
(70) Gardner, J. M.; Beyler, M.; Karnahl, M.; Tschierlei, S.; Ott, S.; Hammarstrom, L. *J. Am. Chem. Soc.* **2012**, *134*, 19322−19325.
(71) Castillo, C. E.; Gennari, M.; Stoll, T.; Fortage, J.; Deronzier, A.; Collomb, M. N.; Sandroni, M.; Legalite, F.; Blart, E.; Pellegrin, Y.; Delacote, C.; Boujtita, M.; Odobel, F.; Rannou, P.; Sadki, S. *J. Phys. Chem. C* **2015**, *119*, 5806−5818.
(72) Kolle, U.; Grutzel, M. *Angew. Chem., Int. Ed. Engl.* **1987**, *26*, 567−570.
(73) Kolle, U.; Kang, B. S.; Infelta, P.; Comte, P.; Gratzel, M. *Chem. Ber.* **1989**, *122*, 1869−1880.
(74) Chardonnoblat, S.; Cosnier, S.; Deronzier, A.; Vlachopoulos, N. *J. Electroanal. Chem.* **1993**, *352*, 213−228.
(75) Cosnier, S.; Deronzier, A.; Vlachopoulos, N. *J. Chem. Soc., Chem. Commun.* **1989**, 1259−1261.
(76) Zhou, X. S.; Dong, Z. R.; Zhang, H. M.; Yan, J. W.; Gao, J. X.; Mao, B. W. *Langmuir* **2007**, *23*, 6819−6826.
(77) Grass, V.; Lexa, D.; Saveant, J. M. *J. Am. Chem. Soc.* **1997**, *119*, 7526−7532.
(78) Arachchige, S. M.; Shaw, R.; White, T. A.; Shenoy, V.; Tsui, H.-M.; Brewer, K. J. *ChemSusChem* **2011**, *4*, 514−518.
(79) Serroni, S.; Juris, A.; Campagna, S.; Venturi, M.; Denti, G.; Balzani, V. *J. Am. Chem. Soc.* **1994**, *116*, 9086−9091.
(80) Canaguier, S.; Field, M.; Oudart, Y.; Pecaut, J.; Fontecave, M.; Artero, V. *Chem. Commun.* **2010**, *46*, 5876−5878.
(81) Felton, G. A. N.; Glass, R. S.; Lichtenberger, D. L.; Evans, D. H. *Inorg. Chem.* **2006**, *45*, 9181−9184.
(82) Zhang, P.; Wang, M.; Gloaguen, F.; Chen, L.; Quentel, F.; Sun, L. *Chem. Commun.* **2013**, *49*, 9455−9457.
(83) Karunadasa, H. I.; Chang, C. J.; Long, J. R. *Nature* **2010**, *464*, 1329−1333.
(84) Dey, S.; Rana, A.; Dey, S. G.; Dey, A. *ACS Catal.* **2013**, *3*, 429−436.
(85) Stoll, T.; Gennari, M.; Serrano, I.; Fortage, J.; Chauvin, J.; Odobel, F.; Rebarz, M.; Poizat, O.; Sliwa, M.; Deronzier, A.; Collomb, M. N. *Chem. - Eur. J.* **2013**, *19*, 782−799.
(86) Delahay, P.; Stiehl, G. L. *J. Am. Chem. Soc.* **1952**, *74*, 3500−3505.
(87) Nicholson, R. S.; Shain, I. *Anal. Chem.* **1964**, *36*, 706.
(88) Saveant, J. M.; Vianello, E. *Electrochim. Acta* **1965**, *10*, 905−920.
(89) Wilson, A. D.; Newell, R. H.; McNevin, M. J.; Muckerman, J. T.; DuBois, M. R.; DuBois, D. L. *J. Am. Chem. Soc.* **2006**, *128*, 358−366.
(90) Elvington, M.; Brewer, K. J. *Inorg. Chem.* **2006**, *45*, 5242−5244.
(91) Yan, S. G.; Brunschwig, B. S.; Creutz, C.; Fujita, E.; Sutin, N. *J. Am. Chem. Soc.* **1998**, *120*, 10553−10554.
(92) Fujita, E.; Brunschwig, B. S.; Creutz, C.; Muckerman, J. T.; Sutin, N.; Szalda, D.; van Eldik, R. *Inorg. Chem.* **2006**, *45*, 1595−1603.
(93) Crabtree, R. H. *Chem. Rev.* **2012**, *112*, 1536−1554.
(94) Vickers, J. W.; Lv, H. J.; Sumliner, J. M.; Zhu, G. B.; Luo, Z.; Musaev, D. G.; Geletii, Y. V.; Hill, C. L. *J. Am. Chem. Soc.* **2013**, *135*, 14110−14118.
(95) Junge, H.; Marquet, N.; Kammer, A.; Denurra, S.; Bauer, M.; Wohlrab, S.; Gartner, F.; Pohl, M. M.; Spannenberg, A.; Gladiali, S.; Beller, M. *Chem. - Eur. J.* **2012**, *18*, 12749−12758.
(96) Anxolabehere-Mallart, E.; Costentin, C.; Fournier, M.; Nowak, S.; Robert, M.; Saveant, J. M. *J. Am. Chem. Soc.* **2012**, *134*, 6104−6107.
(97) El Ghachtouli, S.; Guillot, R.; Brisset, F.; Aukauloo, A. *ChemSusChem* **2013**, *6*, 2226−2230.
(98) Artero, V.; Fontecave, M. *Chem. Soc. Rev.* **2013**, *42*, 2338−2356.
(99) Widegren, J. A.; Finke, R. G. *J. Mol. Catal. A: Chem.* **2003**, *198*, 317−341.
(100) Keene, F. R. *Chem. Soc. Rev.* **1998**, *27*, 185−193.
(101) Patterson, B. T.; Keene, F. R. *Inorg. Chem.* **1998**, *37*, 645−650.
(102) Kew, G.; Hanck, K.; Dearmond, K. *J. Phys. Chem.* **1975**, *79*, 1828−1835.
(103) Allen, G. D.; Buzzeo, M. C.; Villagran, C.; Hardacre, C.; Compton, R. G. *J. Electroanal. Chem.* **2005**, *575*, 311−320.
(104) Labban, A. K. S.; Marcus, Y. *J. Solution Chem.* **1991**, *20*, 221−232.
(105) Costentin, C.; Drouet, S.; Robert, M.; Saveant, J.-M. *J. Am. Chem. Soc.* **2012**, *134*, 11235−11242.
(106) Bakac, A. *Dalton Trans.* **2006**, 1589−1596.
(107) Fourmond, V.; Jacques, P.-A.; Fontecave, M.; Artero, V. *Inorg. Chem.* **2010**, *49*, 10338−10347.
(108) Caix, C.; ChardonNoblat, S.; Deronzier, A. *J. Electroanal. Chem.* **1997**, *434*, 163−170.
(109) Caix, C.; ChardonNoblat, S.; Deronzier, A.; Moutet, J. C.; Tingry, S. *J. Organomet. Chem.* **1997**, *540*, 105−111.
(110) Muckerman, J. T.; Fujita, E. *Chem. Commun.* **2011**, *47*, 12456−12458.
(111) Bhattacharjee, A.; Chavarot-Kerlidou, M.; Andreiadis, E. S.; Fontecave, M.; Field, M. J.; Artero, V. *Inorg. Chem.* **2012**, *51*, 7087−7093.
(112) Marinescu, S. C.; Winkler, J. R.; Gray, H. B. *Proc. Natl. Acad. Sci. U. S. A.* **2012**, *109*, 15127−15131.
(113) Solis, B. H.; Yu, Y. X.; Hammes-Schiffer, S. *Inorg. Chem.* **2013**, *52*, 6994−6999.
(114) Lazarides, T.; McCormick, T.; Du, P.; Luo, G.; Lindley, B.; Eisenberg, R. *J. Am. Chem. Soc.* **2009**, *131*, 9192−9194.
(115) White, T.; Knoll, J.; Arachchige, S.; Brewer, K. *Materials* **2011**, *5*, 27−46.

DOI: 10.1021/acs.inorgchem.5b01536
Inorg. Chem. 2015, 54, 8148−8157